

## Article

# Recycling of Plastic Polymer: Reinforcement of Building Material Using Polymer Plastics of Used COVID-19 Syringes

Golam Fahim \*, Md. Tofazzal Hossain , Stapheny Penheiro, Md. Iffat Bin Zakir, Md. Shamsuzzaman ,  
Mohammad Sarwar Morshed , Sakib Hossain Khan and Abu Hamja

Department of Mechanical and Production Engineering, Ahsanullah University of Science and Technology, Dhaka 1208, Bangladesh

\* Correspondence: fahim.ipe@aust.edu

**Abstract:** Plastic waste causes severe environmental impacts worldwide and threatens the lives of all creatures. In the medical field, most of the equipment, especially personal protective equipment (PPE), is made from single-use plastic. During COVID-19, the usage of PPE has increased, and is disposed of in landfills after being used once. Worldwide, millions of tons of waste syringes are generated from COVID-19 vaccination. A practical alternative to utilizing this waste is recycling it to reinforce building materials. This research introduces an approach to using COVID-19 syringe plastic waste to reinforce building material as composite concrete. Reinforced fiber polymer (FRP) concrete materials were used to mold cylindrical specimens, which underwent mechanical tests for mechanical properties. This study used four compositions with 0%, 5%, 10%, and 15% of FRP to create cylindrical samples for optimum results. Sequential mechanical tests were carried out on the created samples. These specimens were cured for a long period to obtain water absorption capability. After several investigations, the highest tensile and compressive strengths, approximately 2.0 MPa and 10.5 MPa, were found for the 5% FRP composition samples. From the curing test, the lowest water absorbability of around 5% was found for the 5% FRP composition samples.

**Keywords:** COVID-19 plastics; polymer composite; building materials; reinforcement of concrete; recycling of plastics



**Citation:** Fahim, G.; Hossain, M.T.; Penheiro, S.; Zakir, M.I.B.; Shamsuzzaman, M.; Morshed, M.S.; Khan, S.H.; Hamja, A. Recycling of Plastic Polymer: Reinforcement of Building Material Using Polymer Plastics of Used COVID-19 Syringes. *Buildings* **2023**, *13*, 919. <https://doi.org/10.3390/buildings13040919>

Academic Editor: Moncef L. Nehdi

Received: 26 February 2023

Revised: 23 March 2023

Accepted: 27 March 2023

Published: 30 March 2023



**Copyright:** © 2023 by the authors. Licensee MDPI, Basel, Switzerland. This article is an open access article distributed under the terms and conditions of the Creative Commons Attribution (CC BY) license (<https://creativecommons.org/licenses/by/4.0/>).

## 1. Introduction

### 1.1. Usage of Plastics and Their Impacts on the Environment

We can no longer imagine a world without plastics and polymers. All the polymer ever synthesized is still out there somewhere, and it has been a disaster for the ecosystem ever since [1,2]. The onset of the COVID-19 epidemic has only exacerbated the problems associated with managing plastic garbage. The critical situation caused by the COVID-19 epidemic has led to a huge need for personal protective equipment (PPE). Despite the high plastic content, this PPE is the most cost-effective and effective means of preventing the spread of the virus [3]. PPE for health-care systems and frontline employees is necessary, since this virus is spread from person to person via the air. A rise in the detection of symptomless cases has increased the need for PPE kits, particularly single-use items such as face masks, gloves, and face shields.

Consequently, the production and manufacturing of these goods have exploded worldwide [3–6]. Hand gloves, single-use face masks, syringes, eye safety goggles, and disinfectant bottles are some items that divers have lately found floating in the water [7]. Using syringes for COVID-19 vaccinations is inevitable, but they have significant effects on the natural environment. The WHO adopted rules during the epidemic, including using PPE; however, most syringes still wind up in landfills, worsening the environmental consequences [8,9]. The public's adoption of PPE has far-reaching ecological effects beyond its apparent benefits in halting the spread of COVID-19.

The science world has successfully advocated for countermeasures to the COVID-19 pandemic since the pandemic's end, including using repurposing antimicrobial medications to treat affected patients and using attenuated vaccines for protection [10]. According to multiple sources [11,12], the most polluting by-product of mass vaccination centers is a wide variety of mainly nonbiodegradable waste plastics.

The cumulative effect of increased plastic waste on nature during the vaccination campaign or due to routine safety precautions to avoid COVID-19 is enormous and should not be ignored. The prospective use of biodegradable materials, such as bioplastics, may eliminate harmful plastics [11]. Considering the negative environmental consequences caused by discarded COVID-19 vaccines, we provide a vision for creating a sustainable world by utilizing a large number of vaccination syringes to reinforce building materials as an urgent social necessity.

### *1.2. Recycling Plastic for Buildings*

Given the building industry's high material need, recycling polymeric waste into new building materials is one viable option for significantly cutting down on plastic waste. The durability and mechanical characteristics of waste plastics in the building sector must meet the specified applications to guarantee safety and adaptability. Several studies have focused the use of reused plastic wastes in aggregates as a complete or partial substitute for natural aggregates. Successfully combining plastic wastes as fine aggregate, Hama and Hilal [13] created self-consolidating concrete (SCC). According to their findings, adding fine plastic aggregate at a weight percentage of 12.5% may improve the fresh qualities of SCC, such as flow and filling ability. Alqahtani et al. [14], Castillo et al. [15], and Scarpitti et al. [16] studied the feasibility of using recycled waste plastics in lieu of naturally occurring coarse particles in the concrete mixture. In addition, investigators found that the replacement of natural aggregates with greater waste plastics decreased the mechanical parameters (such as compressive, tensile, and flexural strengths, elastic modulus, and water absorptivity). The substitution of coarse and fine aggregates with various waste plastics, namely polypropylene (PP), high-density polyethylene (HDPE), and polyvinyl chloride (PVC), was studied recently by Belmokaddem et al. [17]. Plastic trash was discovered to reduce density dramatically while enhancing acoustical properties in concrete. Synthetic fiber aggregates (PA) were used to replace natural aggregates, and other waste plastics were used as short fibers in fiber-reinforced concrete (FRC). Using a recycled polyethylene terephthalate (PET) container and synthetic waste filament, Khalid et al. [18] carried out a study in FRC. Their experiments using a concrete substrate revealed that increasing the number of fibers and using an unconventional form can significantly improve the lift strengths of synthetic materials. They further implemented their work on a PET-FRC in a constructional beam. Despite their finding that plastic fibers added to concrete had little effect on the mode of failure, they did find that it greatly enhanced the structural capabilities of the beam in terms of cracks and failure strength. Further, Mohammed and Rahim [19] recommended using recycled PET in FRC with high-stress concrete, demonstrating enhanced cracking tolerance afforded by PET fiber. Similarly, Forti and Lerna [20] tested the effects of adding waste PET particles to mortar, finding that the combination increased the mortar's durability.

### *1.3. Alternative Building Materials*

Primarily due to financial constraints, sophisticated synthetic structures in structural engineering application have progressed slowly. Elevated production and raw material costs outweigh their benefits, which include adaptability to a wide variety of shapes and sizes, resistance to corrosion and chemical breakdown in the vast majority of domestic settings, and superior weight-to-strength ratios compared to traditional civil and structural materials. In addition, it is challenging to financially and functionally rationalize using composites in building engineering given the existing practice of component-for-component substitute features in traditional engineering structures with sophisticated laminated composites [21].

Most preexisting concrete buildings suffer from deterioration and degradation throughout their useful lives, making it imperative to reinforce them to enhance structural characteristics and guarantee safety. Fiber-reinforced polymer (FRP) is one of the most popular reinforcement options due to its low density and great corrosion resistance. Aramid FRP (AFRP) and carbon FRP (CFRP) are the most popular FRPs. Still, they are too expensive and have too much of an environmental effect to be practical for application in most nonengineering structures in developing countries, sparking a search for greener alternatives. Recycled waste plastic FRPs (PEN, PET) and natural FRP (cotton, hemp) are only a few examples of environmentally FRP materials that have been developed to date [22–27]. An experimental study by Jirawattansomkul et al. [22,24] found that using environmental FRPs as confinement materials might improve the strength and elasticity of concrete elements. The displacement ductility of concrete components was significantly improved using big-rupture-strain PEN and PET FRPs in investigations of Dai et al. [25,26]. Reinforcing cement using FRPs manufactured from SUP wastes such as plastic syringe waste is uncommon, despite the widespread use of recycled syringe plastics and natural FRPs to replace traditional FRPs. Recycling these SUP scraps into FRP materials instead of throwing them away can benefit land and aquatic environments by reducing the massive annual SUP waste stream.

Even in places where extremes of temperature are common, such as deserts, construction-related projects have been built. In addition to being affected by high temperatures, cement can also fracture from shrinking. The effect of thermal phases on elevated concrete with organic oil palm, polyolefin, and reinforcing steel at varying volumes was studied by Hakeem et al. [28]. The authors demonstrated that fiber insertion in concrete is a common practice when working with FRP composites. This helps to reduce the likelihood of cracking, improve strength development under seismic loading, and boost the structural capacity to absorb shock.

The highly efficient construction composites that use CNTs as supplementary ingredients have a wide range of possible uses [29,30]. Researchers are quickly developing and characterizing nanocomposite materials due to their enthusiasm in nanostructures. Experiments and atomic-level simulations demonstrate that the size influence on mechanical characteristics becomes more important when dealing with nanoscale structures [31]. The impact of CNTs on the bending characteristic of FRP composites was studied by Madenci et al. [29]. The authors used carbon-fiber-reinforced polymer (CFRP), epoxy, and carbon nanotubes (CNTs) in their investigation. The bending behavior of the composites was improved by utilizing 0.3% CNT additions, as shown by a series of mechanical tests conducted by the authors.

The usage of pultruded fiber polymer (PFRP) structures has increased recently in the building trade. These components' behavior changes depending on the location of the web apertures, since they are particularly vulnerable to axial stress. Experimental research was conducted by Madenci et al. [32] employing 21 flexural profiles subjected to vertical stresses, some of which were reinforced with GFRP and CFRP. Based on axial test results, the authors learned that it is crucial to consider the hole's location and quantity when drilling a hole with a particular diameter into a profile. Also, they found that the erratic openings and off-center web apertures drastically cut down on the structure's load-bearing capability. Additionally, a considerable drop in capacity was found when multiple holes were bored together, and reinforcing had the least impact on such specimens. The CFRP specimens were found to yield greater amounts to the samples' load-carrying capability than the GFRP samples.

Creating web holes in building elements is a common requirement for the installation of utility conduits and pipelines. When a building component's  $x$  area is diminished due to webbing, its load-bearing capacity and rigidity are reduced in that location. Experimental research on the impact of web apertures on the behavior of PFRP composite structures to compression load was undertaken by Aksoylu et al. [33]. They examined how the characteristic and durability of PFRP features with fiber-reinforced web apertures varied depending on the hole and the fiber-reinforced scheme. According to their findings, the

width of the holes determines the extent to which the load-bearing ability of specimens is reduced. It turns out that the hole's dimension and the specific CFRP/GFRP strengthening technique used are crucial factors.

The concrete structure used in hydroelectric power plants, which are susceptible to abrasive and erosive action, must be resistant to wear and fracture to ensure their continued regular function and dependability. Polyvinyl alcohol (PVA) fiber combined with magnesium oxide (MgO) expansion agents was utilized in experimental research conducted by Wang et al. [34] to prevent fracturing and abrasion damage. In their research, they explored how adding PVA fiber and MgO to high-strength hydraulic concrete affected its mechanical properties, wear and fracture toughness, pore architectures, and cyclic feature. The authors found that though PVA fiber integration somewhat coarsened the porosity, MgO insertion smoothed the pores.

Important aspects in ensuring the continued regular functioning and stability of cement face earth-fill dams are the concrete's resilience to cracking and its longevity over time. Wang et al. [35] conducted research to determine the effects of fibers of varying lengths (10 mm and 20 mm) made from PP, PVA, and polyacrylonitrile (PAN) on the flowability, resilience, compression behavior, and fracture toughness of the embedded face tile concrete. The scientists showed that PVA > PAN > PP was the most effective sequence for lowering shrinkage and increasing fracture resistance in faced slab concrete. In addition, the inclusion of fibers enhanced the concrete's insulative properties and temperature resistance, with the effectiveness ranking of PAN > PVA > PP.

#### *1.4. Usage of Waste Plastic in Concrete*

As a matter of long-term environmental concern, the replacement of regular Portland cement with reused plastics in specific quantities is an intriguing subject [36–38]. High energy levels are utilized and carbon dioxide (CO<sub>2</sub>) is discharged into the environment during the manufacturing process of cement. As a result, concrete modifiers are of considerable interest [39,40]. The low yield stress as well as the poor tensile strength of regular concrete necessitate the addition of reinforcing bars and occasionally fibers or polymers [41–44]. Although reinforcing bars enhance the mechanical characteristics of concrete, these may not be enough to control crack spread. One of the best methods for limiting crack propagation in concrete structures is the incorporation of fibers [45]. Aside from stopping cracks, fibers are crucial in avoiding the aforementioned negative aspects of concrete [46]. Numerous kinds of fiber can be added to concrete to improve its compressive, bending and resistance to crack [47]. Fibers of many different types are employed in concrete materials, including glass, steel, carbon, etc. [48–52]. Metal scrap, such as old steel parts, is a by-product of modern industry and is categorized as trash since it is produced inefficiently by machining. It is well known that such wastes, in contrast to other wastes, lack a high salvage value and cannot be recycled effectively [53]. It has been discovered [41,54] that the mechanical strength of concrete is increased owing to the use of these scraps as reinforcement. As manufacturing facilities grow, it stands to reason that the quantity of fibers generated by metal businesses would rise as well [55]. Reinforcing fibers, bars, or polymers are used to increase the mechanical strength of building materials [56,57]. Tests have demonstrated that after their first usage, the waste fibers from industries may be recycled into elevated reinforced concrete [58].

In this experimental study, we investigated the contribution of syringe plastic fibers to concrete reinforcement to reduce plastic waste, which causes hazardous effects on our environment. To accomplish this, we mixed varying volume fractions of syringe plastic waste fibers with a certain amount of cement and created several samples to test the mechanical behavior and durability of the resulting reinforced cylindrical blocks. After sequential sampling and mechanical testing, as well as a water-absorbability test, it was found that the volume fraction of 5% of syringe plastic waste provides the best performance compared to the other samples made from a separate waste plastic–concrete mix.

In this experimental study, we investigated the contribution of the syringe plastic fibers to concrete reinforcement, as well as reducing the plastic waste that causes hazardous effects on our environment. To perform this, different volume fractions of syringe plastic waste fibers was mixed with a certain amount of cement and several samples made to test the mechanical behavior as well as the durability of the reinforced cylindrical blocks. After sequential sampling and mechanical testing, as well as a water-absorbability test, it was found that the volume fraction of 5% of syringe plastic waste provides the best performance in comparison to the other samples made from the separate waste plastic–concrete mix.

## 2. Materials and Methods

Many produced SUPs end up in landfills, and COVID-19 immunization syringes are among the most common examples. More and more SPs are being utilized, which poses a threat to ecological systems across the globe. This research includes producing recycled SP as fiber-reinforced composites, studying the microscopic and mechanical features of SP waste fiber-reinforced polymer (SPFRP) composites, and conducting compressive testing on concrete cylinder blocks that SPFRP.

### 2.1. Production of SPFRP

The manufacturing process and the mechanical testing of waste syringe plastic FRP (SPFRP) are shown in Figure 1. The collection of syringes is depicted in Figure 2. Firstly, an overview regarding the waste disposal of used SPs in landfills was studied. The used syringe plastics (SPs) were collected from domestic hospitals and other COVID-19 vaccination campaigns, and then they were cleaned using soapy water, which followed a disinfection step using disinfect sanitizer. Before the disinfection, the injection needle was pulled back wholly into the sheath to prevent the risk of needle sticks. Due to government regulations, disposable syringes, which have nearly identical configurations to COVID vaccination syringes, as seen in Figure 3, were used in this study made by the nongovernmental Indian enterprise GETWELL. Then, the cleaned SPs were wiped with a clean cloth and air-dried for seven days. The dried and cleaned SPs were crushed into tiny plastic particles in a crusher machine. Some of the crushed syringes were mixed with the concrete to form composite FRP.

In this study, 1500 disposable syringes were crushed into tiny plastic particles (Figure 4) in a plastic crusher machine, and 10 kg of crushed plastic was used in different ratios to replace the coarse aggregate. The polypropylene plastic (PP) particles were  $0.5 \pm 0.3$  inches in size. Usually, concrete consists of cement, fine aggregate, coarse aggregate, and water. The coarse aggregates are granular and uneven materials, such as gravel or crushed stone. In this experiment, the coarse aggregate was replaced by 0, 5%, 10%, and 15% (as seen in Table 1) of crushed SPs to optimize the percentage of SPs in the concrete mixture to obtain better mechanical strengths of the FRP. The mixtures of concrete and crushed SPs were poured into the mold and kept for 24 h to create cylindrical blocks. The final products of SPFRPs are shown in Figure 5.

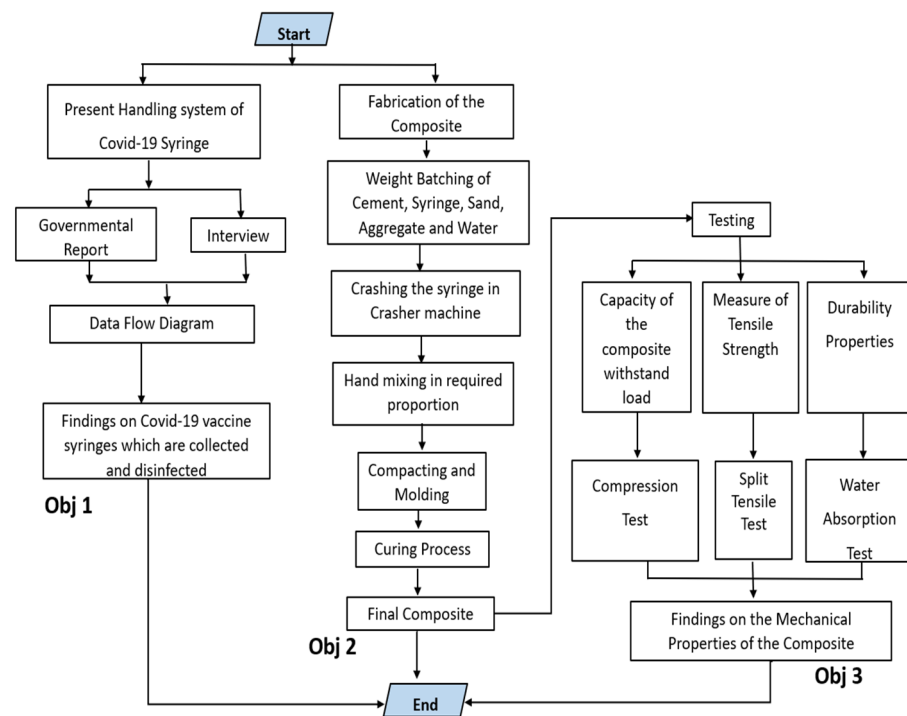


**Figure 1.** Overall workflow diagram of the fabrication of SPFRP composite and mechanical testing procedure.

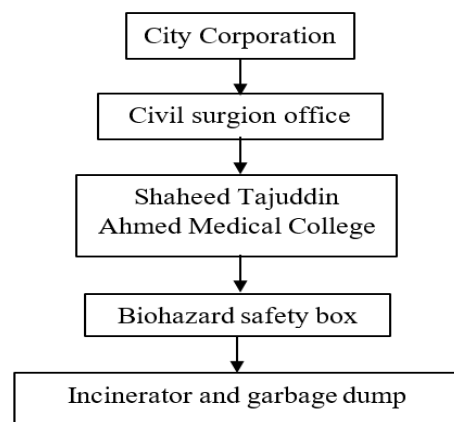


**Figure 2.** Data flow diagram of syringe plastics.



**Figure 3.** Auto-disabled syringes for fixed-dose immunization.



Figure 4. Crushed syringe polypropylene plastic particles.

Table 1. Variation of PP SP percentage in concrete aggregates.

No. of Samples	Percentage of PP SP	Quantity of Cement (kg)	Quantity of Fine Aggregate (kg)	Quantity of PP Plastic (kg)	Quantity of Coarse Aggregate (kg)	Quantity of Water (L)
6	0%			0	18	
6	5%	4	10	0.9	17.1	1.6
6	10%			1.8	16.2	
6	15%			2.7	15.3	



Figure 5. Final cylindrical blocks made of SPFRP.

The final cylindrical samples were created in accordance with the ASTM C31 standard [59]. The mold was cylindrical, with a length and diameter of 8 inches and 4 inches, respectively. Three layers of the concrete mixture were pounded and squeezed into the mold (Figure 6). The samples (Figure 5) were removed from the mold after 24 h and maintained for 28 days to cure (Figure 7). After fixation, various mechanical tests were performed to determine the mechanical properties of the samples after 28 days. Three additional tests—water absorption, compression, and split tensile strength—were performed, and the durability and strength of the composite blocks were identified.



**Figure 6.** Construction of the samples in the cylindrical molds.



**Figure 7.** The samples under the curing process to obtain wettability.

#### 2.1.1. Chemical Properties of the Cement

Ordinary Portland cement (OPC) is used to carry out this experiment. The chemical constituents of OPC are lime (60–67%), silica (17–25%), alumina (3–8%), iron oxide (0.5–6%), magnesia (0.1–4%), sulfur trioxide (1–3%), and soda and potash (0.5–1.3%). Those raw material components undergo chemical reactions during burning and fusing, resulting in tricalcium silicate, dicalcium silicate, tricalcium aluminate, and tetracalcium aluminoferrite compounds.

#### 2.1.2. Purposes of Selecting Design Mixture

The study selected and applied a mix-design approach to make the concrete mixture more uniform and robust, because a concrete mix design takes into account the specifics of the building site and the expected life span of the concrete to determine the optimal ratios of the various constituents. The cement needs for a particular concrete grade at a given location may be lower for a particular technique than it would be for a conventional mix. Compressive testing on cement cylinders assesses the strength of the percentages derived from the concrete mix design.

The resulting building will be as sturdy as possible when the material is mixed properly. It also helps us get the most out of our concrete by minimizing waste and making the most of our dry and wet components.

Mix design aims to determine the relative quantities of ingredients that will provide concrete with the desired characteristics. The mix proportions should be chosen such that the resultant concrete has the appropriate workability when fresh, and can be conveniently put and pressed for the purpose desired. The concrete, while still wet, must be fluid enough to fill it up the concrete slabs and encapsulate the reinforcing, and after it has been set, it must be strong and durable enough to meet the project's needs.

The efficacy of the fibers was measured using a series of experiments designed to probe several properties of SPFRP concrete. We may adjust the SP fiber content by adding more or less to the concrete mix. Elevated SPFRP fiber concrete was produced in this research using 0, 5%, 10%, and 15% SP fibers by the amount of concrete used. The SP fiber and cement were used to create four different blends. An experimental investigation was conducted to determine the varying mechanical properties of the elevated SPFRP fibrous polymer using cylinders with diameters of 97 mm, 101 mm, 101.5 mm, 102 mm, and 103 mm.

### 3. Experimental Procedures

In this research, three sorts of mechanical testing of the specimens—water-absorption test, compression test, and split tensile strength test—were conducted to identify the composite's durability and mechanical strengths.

#### 3.1. Water-Absorption Test

Water-absorption testing is one of the most common methods to evaluate the water tightness of concrete. It is the term for fluid flow in porous media such as concrete under saturated circumstances and without external pressure. The amount of water that permeates concrete samples while submerged is measured using this method to determine water-absorption capability. Before testing, 8 × 4-inch specimens were dried for 30 min at room temperature to make the specimens moisture free. The specimens were then fully submerged in water for 28 days. After this time, the specimens were taken out and dried at ambient temperature for an hour to remove water from their surfaces. Then, the weights of the saturated samples were measured using an analytical weighing balance, and after that they were dried in an oven at 110 °C for 24 h. After being dried in the oven, the weights were further measured. Finally, the percentage of water absorbed ( $W_{ab}$ ) was found using Equation (1).

$$W_{ab} = \frac{(W_w - W_d)}{W_d} \times 100\% \quad (1)$$

$W_w$  is the samples' weight at the saturated condition, and  $W_d$  is the weight of the dried samples. The experimental procedures are shown in Figure 8.

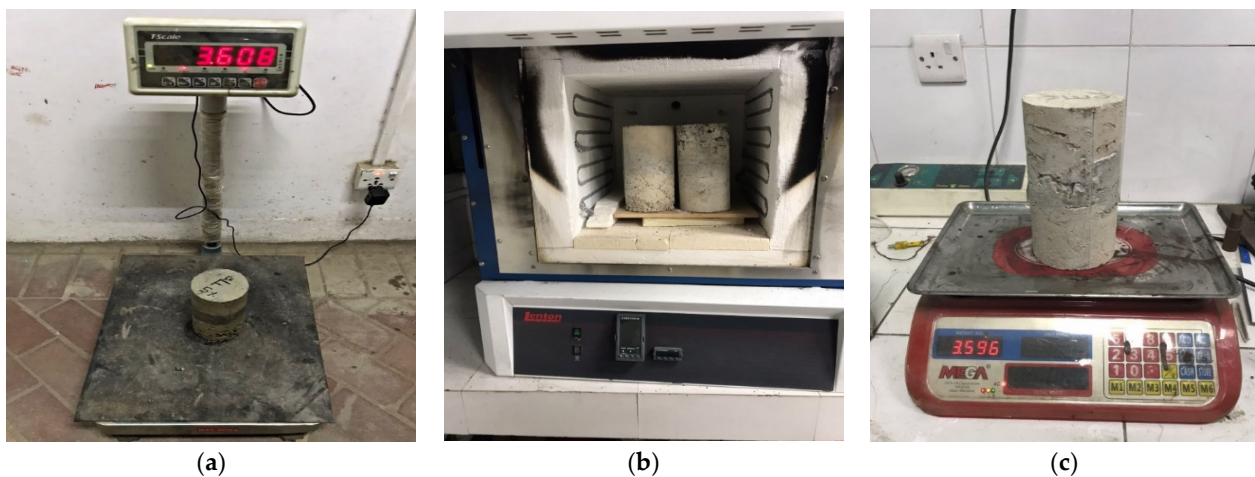


**Figure 8.** Weight measurements of the dry and wet samples: (a) wet condition weight, (b) drying process, and (c) dry condition weight.

### 3.2. Compression Test

The compression test was performed with the help of a universal testing machine (UTM) operated manually according to ASTM C31 [59]. In the compression test, a total of 8 cylindrical specimens were used. Before the test, the specimens were pulled out from the water after the specified curing time, and excess water was wiped out from the surfaces. With the help of slide calipers, the dimensions of the cylindrical blocks were measured to find out the surface area. The geometrical measurements are given in Table 2.

**Table 2.** Geometrical characteristics of the specimens for compression test.

Percentage of Syringe Plastic in Composites	Sample ID	Diameter (mm)	Radius (mm)	Section Area (mm <sup>2</sup> )
0%	D	101.33	50.67	8067
	B	101.54	50.77	8100
5%	D	102.22	51.11	8209
	C	102.85	51.43	8311
10%	B	102.78	51.39	8300
	C	102.09	51.05	8189
15%	D	101.58	50.79	8107
	C	97.01	51.68	7394

At first, the flat surfaces of the specimen were placed in the machine in such a manner that the load was applied to the opposite sides of the cylinder cast, as shown in Figure 9. The pressure was increased gradually with respect to time until the failure of the sample appeared to find the maximum load. Equation (2) was used to determine the compression strength of the specimens.

$$\sigma_c = \frac{F}{\pi r^2} \quad (2)$$

where  $\sigma_c$  is compression strength in MPa,  $F$  is the maximum load in Newtons (N), and  $r$  is the radius of each specimen in mm<sup>2</sup>.



(a)



(b)

**Figure 9.** Experimental setup for compression test of the cylindrical samples: (a) placement of the specimen in the UTM, and (b) failure of the specimens under compression.

### 3.3. Split Tensile Test

The split tensile tests of the 8 specimens were performed following ASTM C496 [59] instructions with the help of the UTM with a capacity of 800 kN. After the required curing

time (28 days), the specimens were taken out of the water, and any excess water was dried off the surface. In this experiment, the load was applied at a constant rate of 3 mm/min. The tensile splitting strength was found using Equation (3). The experimental procedures of this tensile test are shown in Figure 10.

$$\sigma_t = \frac{2F}{\pi Ld} \quad (3)$$

where  $\sigma_t$  is tensile splitting strength in MPa,  $F$  is the maximum load in N,  $L$  is the length of the specimen in mm, and  $d$  is the diameter of the specimen in mm.

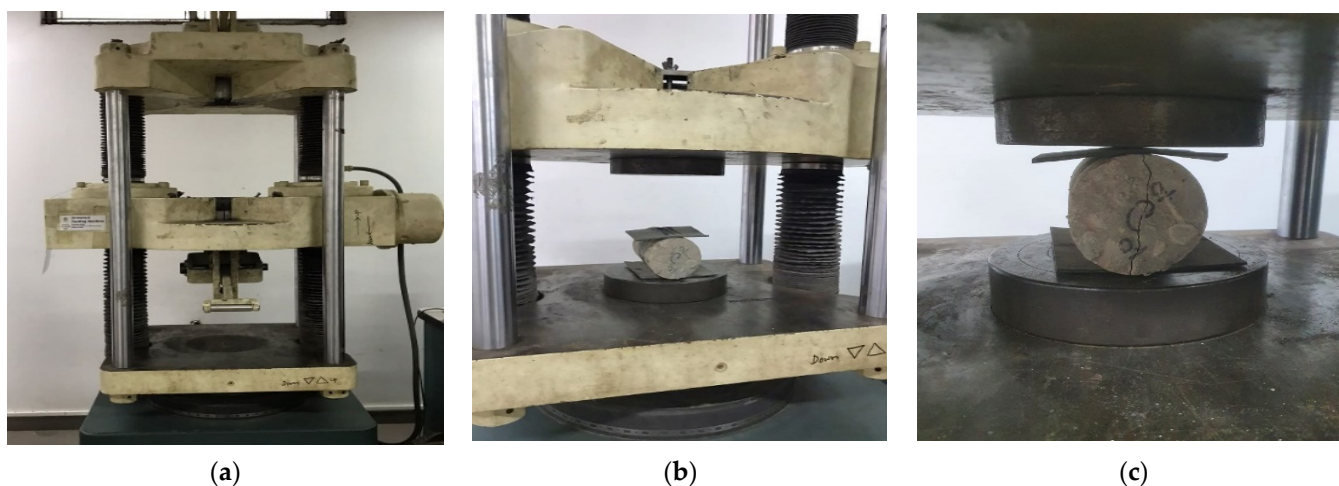


**Figure 10.** Experimental setup for split tensile test of the cylindrical samples: (a) UTM for tensile splitting strength, (b) placement of the specimen in UTM, and (c) specimen after failing under tensile splitting strength.

## 4. Results and Discussion

### 4.1. Water-Absorption Test

The salient features of the pore structures in concrete, absorption characteristics, as well as concrete's durability, can be revealed with the help of the water-absorption rate of concrete. Correlations among the indices of water absorption and other corrosive parameters of concrete can also be developed using this water-absorption test, as found in previous studies. The results of the water-absorption test are shown in Table 3 and Figure 11.

**Table 3.** Average water absorption rate in different specimens.

Amount of Plastic (%)	Specimen	Weight of Dry Block, $W_d$ (kg)	Weight of Wet Block, $W_w$ (kg)	Water Absorption, $W_{ab}$ (%)	Average Water Absorption, $W_{ab}$ (%)
0%	E	3.596	3.754	4.393	4.652
	F	3.726	3.909	4.911	
5%	E	3.444	3.633	5.487	4.942
	F	3.456	3.608	4.398	
10%	A	3.144	3.364	6.997	6.375
	E	3.320	3.511	5.753	
15%	A	2.806	3.029	7.947	7.91
	E	2.80	3.021	7.892	

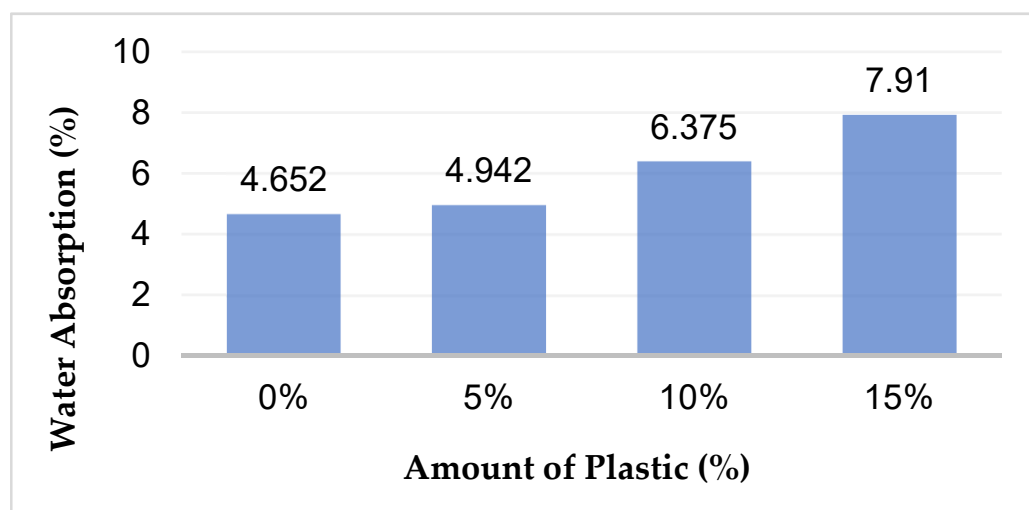


**Figure 11.** Variation of water absorption with the changes in plastic percentage in the composite concrete.

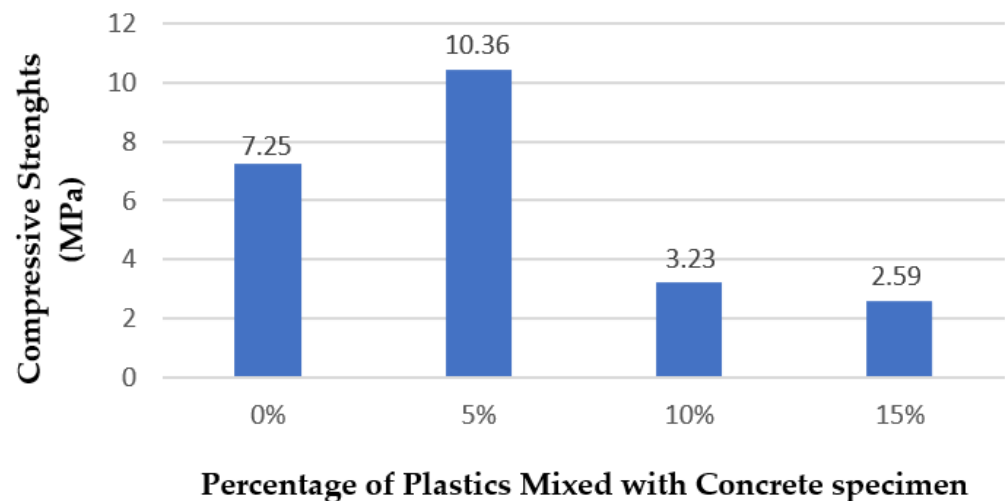
The impact of aggregate on concrete can be influenced either by the variation in the intensity of porosity or the variation in the paste. The percentage of water absorption for different specimens has been illustrated in Table 3. In addition, the variations in the water absorption capacity of the cylindrical blocks have been visualized with the changes in plastic percentage in the reinforced composite blocks. It is seen that the percentage of water absorption in the SPFRP cylindrical blocks increased due to the addition of plastic aggregate in the concretes. The highest water absorption was found for the 15% plastic aggregate in the concrete. From this finding, it can be said that the number of inclusions or pores increases with the addition of SP in concretes. The increase in water absorption may be attributed to weak bonding in the concrete mixtures, which could be made more difficult by the presence of plastic aggregate to form a stronger bond with the cement, thereby allowing water to pass through more easily. Therefore, increased plastic aggregate in concrete causes an increase in water absorption as well as a decrease in the durability of concrete, because a concrete mixture with excessive water may crack. Moreover, excessive water and plastic inclusions in concrete might cause dusting, pop-outs, and moisture-absorption increase in concrete.

#### 4.2. Compression Test

Table 4 shows the compressive loads and the ultimate compressive strengths up to the failure of the specimens found in the compression test. It is seen that the ultimate compressive strength decreases with the addition of plastics (PP) to replace the coarse aggregate in concrete after a 5% mix of SP. It is also clear from Figure 12 that the maximum compressive strength (10.36 MPa) was found for the sample of 5% SP mixed with the concrete. This might be caused due to the poor bonding between the plastic's surface and the cement's binder at a higher percentage of plastics. To avoid this failure, it is suggested to optimize the usage of plastic concentrations in the concrete mix. In Figure 13, the compression load variations in the specimens are shown with time until the failure of the specimens. The highest compressive failure time (170 s) was found in the sample of 5% SP mix in concrete.

**Table 4.** Maximum compressive force and ultimate compressive strengths of the specimens found in the compression test.

Amount of Plastic (%)	Sample ID	Section Area, A (mm <sup>2</sup> )	Maximum Force, F (kN)	Ultimate Compressive Strength, $\sigma_c$ (MPa)
0%	B0	8100	55.90	6.9
	D0	8067	61.00	7.6
5%	C5	8311	93.60	11.3
	D5	8209	77.65	9.5
10%	B10	8300	32.25	3.9
	C10	8189	21.15	2.6
15%	C15	7394	21.95	3.0
	D15	8107	18.15	2.2

**Figure 12.** Variation of compressive strengths with the changes in plastic percentage in the composite concrete.

From Figure 14, the variation of tensile strength with the percentage of SP fiber in concrete can be correlated using the following equation (Equation (4)).

$$\sigma_c = -0.42v_f + 9.02 \quad (4)$$

where  $v_f$  is the volume fraction of SP fiber in concrete in percentage and  $\sigma_c$  is the ultimate tensile strength in MPa of SPFRP concrete.

In this experiment, the compressive strengths were 7.25 MPa for 0 SP mix, 10.4 MPa for 5% SP mix, 3.25 MPa for 10% SP mix, and 2.6 MPa for 15% SP mix found. Therefore, based on the finding above and an average of the results for various SP mix ratios, the 5% plastic replacement with coarse aggregate exhibits higher compressive strength.

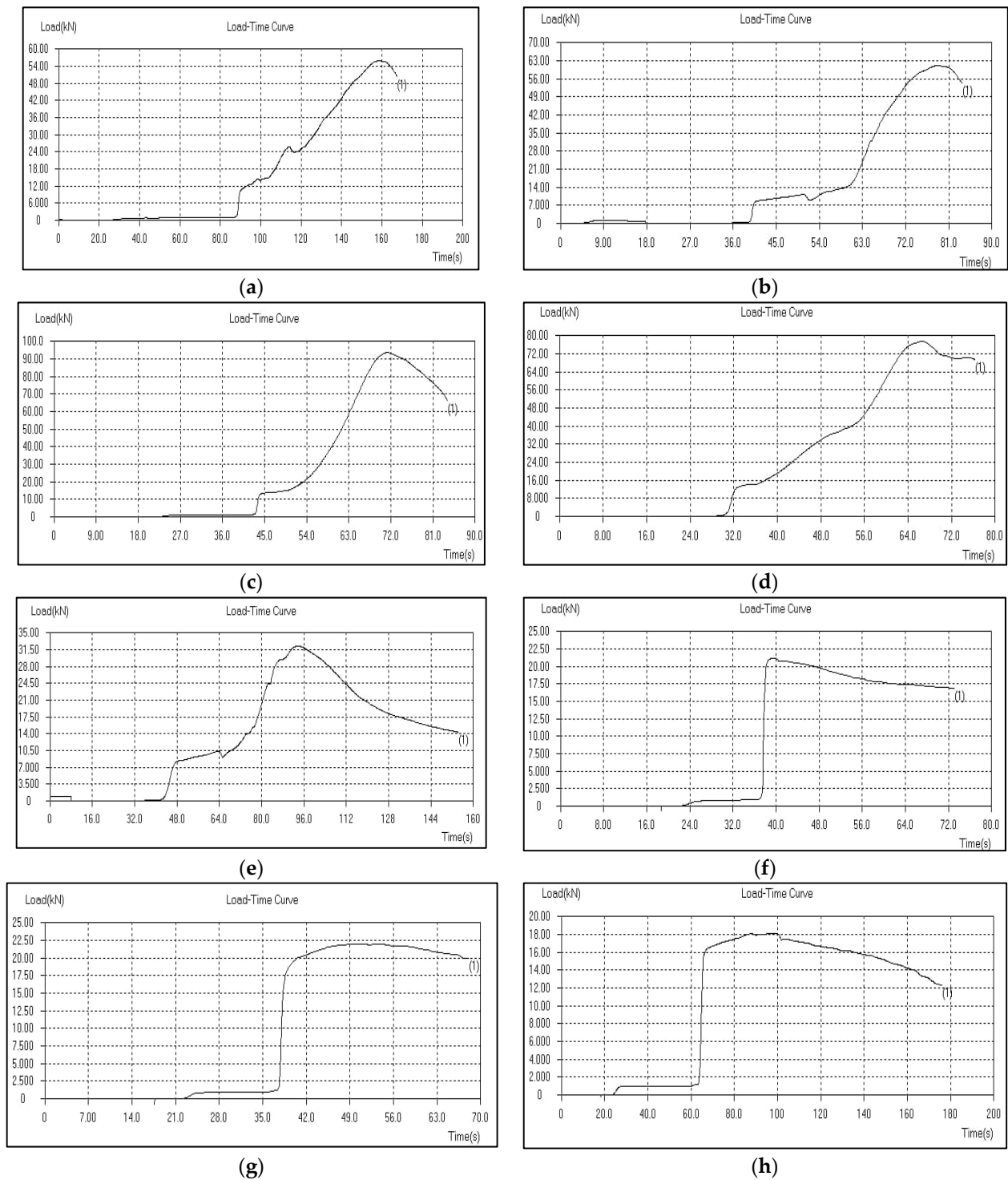


**Figure 13.** Load–time curve for different cylindrical specimens from the compressive tests in a UTM with sample ID of (a) B0, (b) D0, (c) C5, (d) D5, (e) B10, (f) C10, (g) C15, and (h) D15.

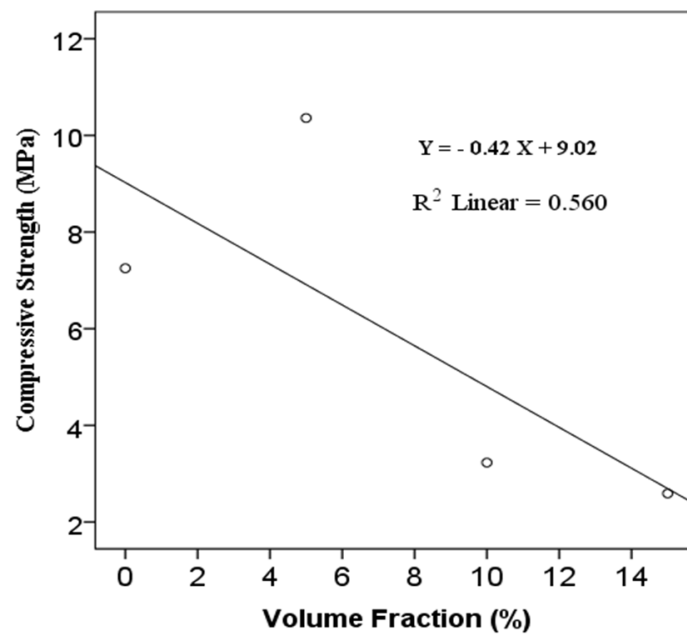


**Figure 14.** Correlation between the ultimate compressive strength and the volume fraction percentage of SPFRP in concrete.

#### 4.3. Split Tensile Test

Table 5 shows the split tensile loads and the ultimate tensile strengths up to the failure of the specimens found in the split tensile test. It is seen that the ultimate tensile strength decreases with the addition of plastics (PP) to replace the coarse aggregate in concrete after a 5% mix of SP. It is also clear from Figure 15 that the maximum tensile strength (1.934 MPa) was for the sample of 5% SP mix with the concrete. This might be caused due to the poor bonding between the plastic's surface and the cement's binder at a higher percentage of plastics. To avoid this failure, it is suggested to optimize the usage of plastic concentrations in the concrete mix.

**Table 5.** Maximum tensile force and ultimate tensile strengths of the specimens found in the split tensile test.

Amount of Plastic (%)	Sample ID	Tensile Load, F (kN)	Average Tensile Load, F (kN)	Ultimate Tensile Strength, $\sigma_t$ (MPa)
0%	A	55.451	56.38	1.761
	C	57.309		
5%	A	37.79	61.905	1.934
	B	61.905		
10%	D	20.275	22.987	0.718
	F	25.7		
15%	B	24.052	18.55	0.579
	F	13.061		

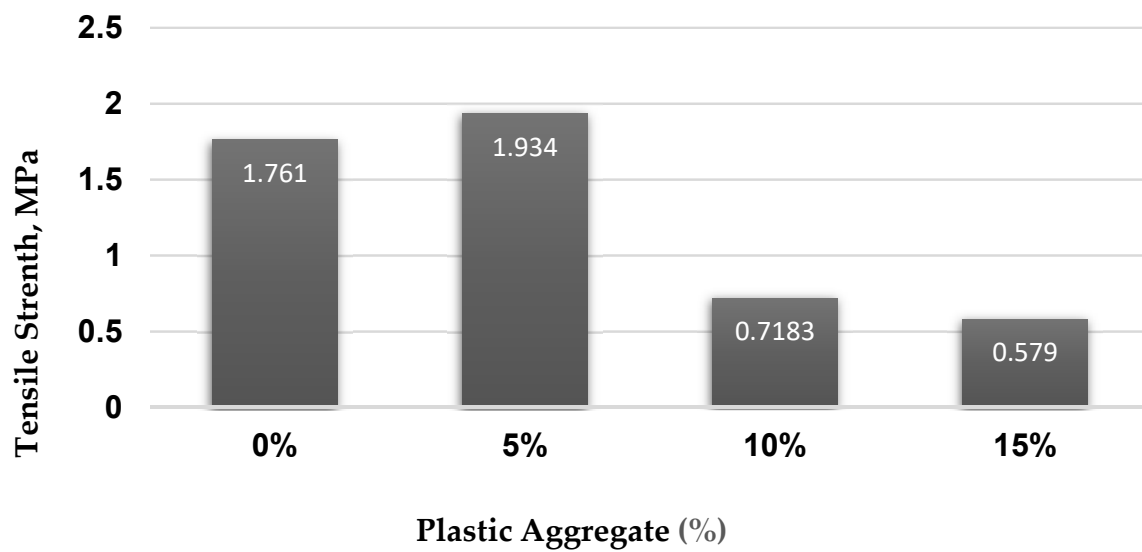


**Figure 15.** Variation of split tensile strength with the changes in plastic percentage in the composite concrete.

For 5% plastic aggregate, an unusual load of 37.79 kN appeared for specimen A, which might be caused due to uneven tempering or construction fault. For this, the value of 5% (specimen A) has been disregarded so far.

From Figure 16, the variation of tensile strength with the percentage of SP fiber in concrete can be correlated using the following equation (Equation (5)).

$$\sigma_t = -0.1v_f + 1.96 \quad (5)$$

where  $v_f$  is the volume fraction of SP fiber in concrete in percentage and  $\sigma_t$  is the ultimate tensile strength of SPFRP concrete.

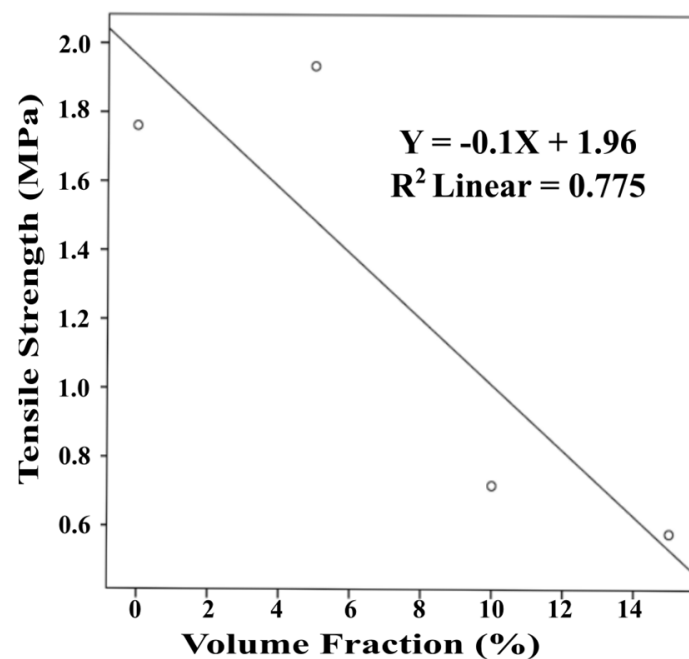


**Figure 16.** Correlation between the ultimate tensile strength and the volume fraction percentage of SPFRP in concrete.

The tensile strengths for the specimens of 0 and 5% plastic aggregate were 1.761 MPa and 1.934 MPa, which is a slight increase. However, the tensile strength significantly decreased for the 10% and 15% SP mixtures. Since the bindings between cement and aggregate are stronger than those between cement and plastic aggregate, adding more plastic particles causes a weaker binding. Therefore, split tensile strength decreases after reaching an optimum condition, and the SPFRP becomes weaker.

#### 4.4. Analysis of Standard and Experimental Values

The experimental water-absorption rate is shown in Figure 17 to compare with the ASTM C39 standard [59] water-absorption rate of the concrete structure. Though the water absorption rate rises in concrete with the mixture of SP aggregate, the ASTM standard suggests that the 0–10% SP aggregates in concrete might be useful. Beyond this limit of SP mix, excessive inclusions or porosity in concrete might cause concrete failure, and the mechanical strength of the concrete will be adversely affected. Other than that, the 15% plastic mix shows a higher rate of water absorption, and more water absorption reduces the workability of the concrete.

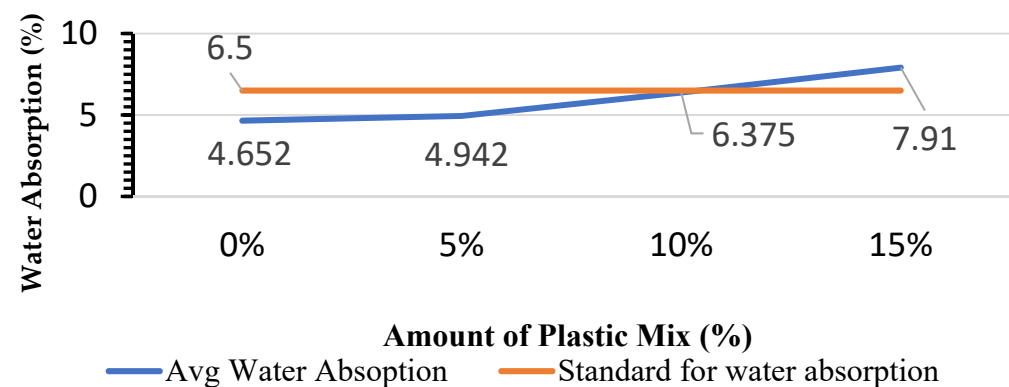


Figure 17. Comparison of water absorption with standard value.

According to ASTM C39 [59], the standard value for compressive strength of concrete is in the range of 8 MPa to 40 MPa. In this experiment, the highest value of compressive strength of 10.36 MPa was found for the 5% of SP mix in concrete. Therefore, this 5% mix SPFRP concrete can be a viable alternative to concrete aggregate in building materials. On the other hand, the split tensile strength of the concrete structure is about 10% of the compressive strength. The results of split tensile strength were nearly consistent, as shown in Figure 18.

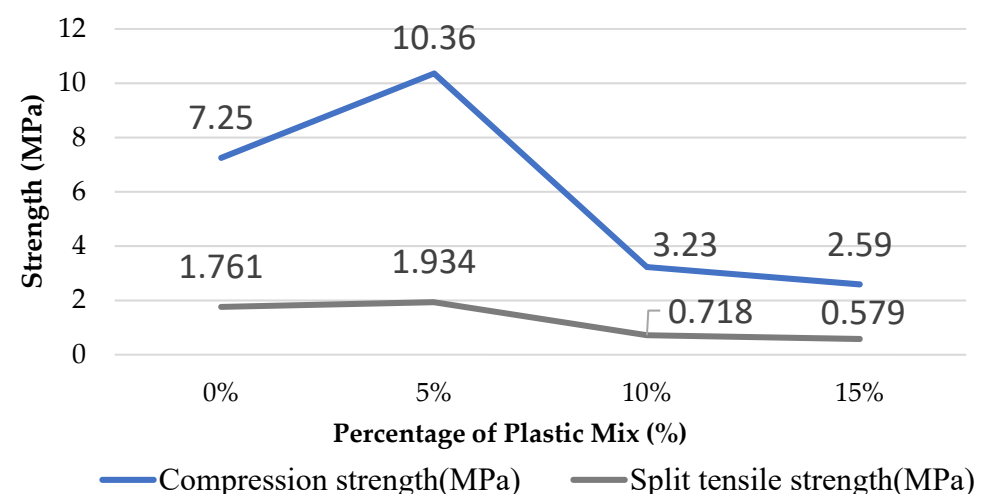


Figure 18. Strength for different percentages of plastic aggregation.

## 5. Conclusions

The major goal of this study was to pioneer the production of a syringe plastic fiber-reinforced polymer (SPFRP) for use in concrete confinement. Concrete cylinder block properties such as water absorption, compressive strength, and split tensile strength were examined to ascertain the effect of SPFRP confinement. The percentage of syringe plastic used (5–15%) as aggregate in concrete samples is the most important variable to consider. An environmental impact assessment was conducted to determine the SPFRP's viability. The following is a summary of the findings.

1. The COVID-19 pandemic has led to a rise in the use of disposable plastics; thus, it is essential to reduce their accumulation via recycling in favor of the usage of new plastics. A simple manufacturing method might be used by people to create FRP from discarded plastic syringes. The mechanical qualities of SPFRP, including ultimate compressive strength and ultimate tensile strength, are adequate for strengthening from an engineering perspective. As the syringe plastic's surface might weaken the binding between aggregate and concrete, it is unclear how to keep the volume percentage of syringe plastics and concrete uniform. This indicates that uniform mixing of the syringe plastic aggregate with the concrete will increase both the bonding strength and hence the mechanical strength of the SPFRP.
2. It was found that the mechanical properties of the FRP were significantly affected due to the mixing of syringe plastics fiber with concrete beyond a certain percentage of plastic fiber. This study aimed to find an alternative that can overcome the plastic wastes for the sustainability of our environment and can be utilized as a concrete material for low-load-bearing applications such as cement-based plaster with SPFRP confinement to cover and smoothen the surface of walls and ceilings, flooring in garages, warehouses, and industrial facilities, as well as grouts to fill gaps between tiles, bricks, or other building materials. In addition, it can be used for the casting of varieties of blocks, pavers, and decorative elements in landscaping and construction projects.
3. In terms of durability, concrete's compressive strength enhancement due to SPFRP confinement increased from 7.25% to 10.36% with a five percent (5% *w/w*) SP aggregate mix. The concrete can benefit greatly from the SPFRP confinement's reinforcing effect.
4. Concerning environmental effects, SPFRP may greatly minimize the quantity of plastic syringe waste. In this study, reinforcement of eight concrete cylinder blocks may reduce the total of 1500 syringe plastics, suggesting successful waste management by reusing used syringe plastics. The real reinforcing of reinforced concrete columns needs greater strengthening regions than in a small-scale concrete cylinder test, meaning higher requirement for SP wastes. Continued deployment of SPFRP strengthening in real full-scale columns should be carefully undertaken to determine its usability and to analyze the environmental effects.

**Author Contributions:** Conceptualization, G.F., M.S.M. and A.H.; Methodology, G.F.; Software, M.I.B.Z. and M.S.; Validation, S.P.; Formal analysis, M.T.H., M.S.M. and S.H.K.; Investigation, M.I.B.Z., M.S., M.S.M. and S.H.K.; Resources, S.P., M.I.B.Z. and M.S.; Data curation, M.T.H., S.P. and S.H.K.; Writing—original draft, G.F. and M.T.H.; Writing—review & editing, A.H. All authors have read and agreed to the published version of the manuscript.

**Funding:** This research received no external funding.

**Conflicts of Interest:** The authors declare no conflict of interest.

## References

1. Geyer, R.; Jambeck, J.R.; Law, K.L. Production, use, and fate of all plastics ever made. *Sci. Adv.* **2017**, *3*, e1700782. [[CrossRef](#)]
2. Inamdar, I. Recycling of plastic wastes generated from COVID-19: A comprehensive illustration of type and properties of plastics with remedial options. *Sci. Total Environ.* **2022**, *838*, 155895. [[CrossRef](#)]

3. Vanapalli, K.R.; Sharma, H.B.; Ranjan, V.P.; Samal, B.; Bhattacharya, J.; Dubey, B.K.; Goel, S. Challenges and strategies for effective plastic waste management during and post COVID-19 pandemic. *Sci. Total Environ.* **2021**, *750*, 141514. [[CrossRef](#)]
4. Yudell, M.; Roberts, D.; DeSalle, R.; Tishkoff, S. NIH must confront the use of race in science. *Science* **2020**, *369*, 1314–1315. [[CrossRef](#)]
5. Prata, J.C.; Silva, A.L.P.; Walker, T.R.; Duarte, A.C.; Rocha-Santos, T. COVID-19 Pandemic Repercussions on the Use and Management of Plastics. *Environ. Sci. Technol.* **2020**, *54*, 7760–7765. [[CrossRef](#)] [[PubMed](#)]
6. Parashar, N.; Hait, S. Plastics in the time of COVID-19 pandemic: Protector or polluter? *Sci. Total Environ.* **2021**, *759*, 144274. [[CrossRef](#)] [[PubMed](#)]
7. Roberts, K.; Bowyer, C.; Kolstoe, S.; Fletcher, S. Coronavirus Face Masks: An Environmental Disaster that Might Last Generations. 2020. Available online: <https://theconversation.com/coronavirus-face-masks-an-environmental-disaster-that-might-last-generations-144328> (accessed on 21 February 2023).
8. Saberian, M.; Li, J.; Kilmartin-Lynch, S.; Boroujeni, M. Repurposing of COVID-19 single-use face masks for pavements base/subbase. *Sci. Total Environ.* **2021**, *769*, 145527. [[CrossRef](#)] [[PubMed](#)]
9. Sangkham, S. Face mask and medical waste disposal during the novel COVID-19 pandemic in Asia. *Case Stud. Chem. Environ. Eng.* **2020**, *2*, 100052. [[CrossRef](#)]
10. Klemeš, J.J.; Jiang, P.; Van Fan, Y.; Bokhari, A.; Wang, X.C. COVID-19 pandemics Stage II—Energy and environmental impacts of vaccination. *Renew. Sustain. Energy Rev.* **2021**, *150*, 111400. [[CrossRef](#)]
11. Hasija, V.; Patial, S.; Raizada, P.; Thakur, S.; Singh, P.; Hussain, C.M. The environmental impact of mass coronavirus vaccinations: A point of view on huge COVID-19 vaccine waste across the globe during ongoing vaccine campaigns. *Sci. Total Environ.* **2022**, *813*, 151881. [[CrossRef](#)]
12. Baumann, N.; Chen, S.; McDonald, J.R.; Davis, M.H.; Petroff, C.; McKelvy, P. Mitigating COVID-19 Vaccine Waste through a Multidisciplinary Inpatient Vaccination Initiative. *J. Healthc. Qual.* **2022**, *44*, 178–183. [[CrossRef](#)] [[PubMed](#)]
13. Hama, S.M.; Hilal, N.N. Fresh properties of self-compacting concrete with plastic waste as partial replacement of sand. *Int. J. Sustain. Built Environ.* **2017**, *6*, 299–308. [[CrossRef](#)]
14. Alqahtani, F.K.; Ghataora, G.; Khan, M.I.; Dirar, S. Novel lightweight concrete containing manufactured plastic aggregate. *Constr. Build. Mater.* **2017**, *148*, 386–397. [[CrossRef](#)]
15. del Rey Castillo, E.; Almesfer, N.; Saggi, O.; Ingham, J.M. Light-weight concrete with artificial aggregate manufactured from plastic waste. *Constr. Build. Mater.* **2020**, *265*, 120199. [[CrossRef](#)]
16. Scarpitti, N.; Gavio, N.; Pol, A.; Sanei, S.H. Recycling Unrecycled Plastic and Composite Wastes as Concrete Reinforcement. *J. Compos. Sci.* **2023**, *7*, 11. [[CrossRef](#)]
17. Belmokaddem, M.; Mahi, A.; Senhadji, Y.; Pekmezci, B.Y. Mechanical and physical properties and morphology of concrete containing plastic waste as aggregate. *Constr. Build. Mater.* **2020**, *257*, 119559. [[CrossRef](#)]
18. Khalid, F.S.; Irwan, J.M.; Wan Ibrahim, M.H.; Othman, N.; Shahidan, S. Splitting tensile and pullout behavior of synthetic wastes as fiber-reinforced concrete. *Constr. Build. Mater.* **2018**, *171*, 54–64. [[CrossRef](#)]
19. Mohammed, A.A.; Rahim, A.A.F. Experimental behavior and analysis of high strength concrete beams reinforced with PET waste fiber. *Constr. Build. Mater.* **2020**, *244*, 118350. [[CrossRef](#)]
20. Foti, D.; Lerna, M. New Mortar Mixes with Chemically Depolymerized Waste PET Aggregates. *Adv. Mater. Sci. Eng.* **2020**, *2020*, 8424936. [[CrossRef](#)]
21. Van Den Einde, L.; Zhao, L.; Seible, F. Use of FRP composites in civil structural applications Lelli. *Constr. Build. Mater.* **2003**, *17*, 389–403. [[CrossRef](#)]
22. Jirawattanasomkul, T.; Ueda, T.; Likitlersuang, S.; Zhang, D.; Hanwiboonwat, N.; Wuttiwannasak, N.; Horsangchai, K. Effect of natural fibre reinforced polymers on confined compressive strength of concrete. *Constr. Build. Mater.* **2019**, *223*, 156–164. [[CrossRef](#)]
23. Jirawattanasomkul, T.; Likitlersuang, S.; Wuttiwannasak, N.; Ueda, T.; Zhang, D.; Shono, M. Structural behaviour of pre-damaged reinforced concrete beams strengthened with natural fibre reinforced polymer composites. *Compos. Struct.* **2020**, *244*, 112309. [[CrossRef](#)]
24. Jirawattanasomkul, T.; Likitlersuang, S.; Wuttiwannasak, N.; Ueda, T.; Zhang, D.; Voravutvityaruk, T. Effects of Heat Treatment on Mechanical Properties of Jute Fiber-Reinforced Polymer Composites for Concrete Confinement. *J. Mater. Civ. Eng.* **2020**, *32*, 04020363. [[CrossRef](#)]
25. Dai, J.-G.; Bai, Y.-L.; Teng, J.G. Behavior and Modeling of Concrete Confined with FRP Composites of Large Deformability. *J. Compos. Constr.* **2011**, *15*, 963–973. [[CrossRef](#)]
26. Dai, J.G.; Lam, L.; Ueda, T. Seismic retrofit of square RC columns with polyethylene terephthalate (PET) fibre reinforced polymer composites. *Constr. Build. Mater.* **2012**, *27*, 206–217. [[CrossRef](#)]
27. Rousakis, T.C. Reusable and recyclable nonbonded composite tapes and ropes for concrete columns confinement. *Compos. Part B Eng.* **2016**, *103*, 15–22. [[CrossRef](#)]
28. Hakeem, I.; Hosen, M.A.; Alyami, M.; Qaidi, S.; Özkılıç, Y. Influence of Heat-Cool Cyclic Exposure on the Performance of Fiber-Reinforced High-Strength Concrete. *Sustainability* **2023**, *15*, 1433. [[CrossRef](#)]
29. Madenci, E.; Özkılıç, Y.O.; Aksoylu, C.; Asyraf, M.R.M.; Syamsir, A.; Supian, A.B.M.; Mamaev, N. Buckling Analysis of CNT-Reinforced Polymer Composite Beam Using Experimental and Analytical Methods. *Materials* **2023**, *16*, 614. [[CrossRef](#)]

30. Thostenson, E.T.; Ren, Z.; Chou, T.W. Advances in the science and technology of carbon nanotubes and their composites: A review. *Compos. Sci. Technol.* **2001**, *61*, 1899–1912. [[CrossRef](#)]
31. Wuite, J.; Adali, S. Deflection and stress behaviour of nanocomposite reinforced beams using a multiscale analysis. *Compos. Struct.* **2005**, *71*, 388–396. [[CrossRef](#)]
32. Madenci, E.; Özkılıç, Y.O.; Aksoylu, C.; Safonov, A. The Effects of Eccentric Web Openings on the Compressive Performance of Pultruded GFRP Boxes Wrapped with GFRP and CFRP Sheets. *Polymers* **2022**, *14*, 4567. [[CrossRef](#)] [[PubMed](#)]
33. Aksoylu, C.; Özkılıç, Y.O.; Madenci, E.; Safonov, A. Compressive Behavior of Pultruded GFRP Boxes with Concentric Openings Strengthened by Different Composite Wrappings. *Polymers* **2022**, *14*, 4095. [[CrossRef](#)] [[PubMed](#)]
34. Wang, L.; Zeng, X.; Li, Y.; Yang, H.; Tang, S. Influences of MgO and PVA Fiber on the Abrasion and Cracking Resistance, Pore Structure and Fractal Features of Hydraulic Concrete. *Fractal Fract.* **2022**, *6*, 674. [[CrossRef](#)]
35. Wang, L.; He, T.; Zhou, Y.; Tang, S.; Tan, J.; Liu, Z.; Su, J. The influence of fiber type and length on the cracking resistance, durability and pore structure of face slab concrete. *Constr. Build. Mater.* **2021**, *282*, 122706. [[CrossRef](#)]
36. Zeybek, Ö.; Özkılıç, Y.O.; Karalar, M.; Çelik, A.İ.; Qaidi, S.; Ahmad, J.; Burduhos-Nergis, D.D.; Burduhos-Nergis, D.P. Influence of Replacing Cement with Waste Glass on Mechanical Properties of Concrete. *Materials* **2022**, *15*, 7513. [[CrossRef](#)] [[PubMed](#)]
37. Batayneh, M.; Marie, I.; Asi, I. Use of selected waste materials in concrete mixes. *Waste Manag.* **2007**, *27*, 1870–1876. [[CrossRef](#)]
38. Jiang, X.; Xiao, R.; Bai, Y.; Huang, B.; Ma, Y. Influence of waste glass powder as a supplementary cementitious material (SCM) on physical and mechanical properties of cement paste under high temperatures. *J. Clean. Prod.* **2022**, *340*, 130778. [[CrossRef](#)]
39. Tayeh, B.A.; Al Saffar, D.M.; Aadi, A.S.; Almeshal, I. Sulphate resistance of cement mortar contains glass powder. *J. King Saud Univ. Eng. Sci.* **2020**, *32*, 495–500. [[CrossRef](#)]
40. Tayeh, B.A.; Almeshal, I.; Magbool, H.M.; Alabduljabbar, H.; Alyousef, R. Performance of sustainable concrete containing different types of recycled plastic. *J. Clean. Prod.* **2021**, *328*, 129517. [[CrossRef](#)]
41. Çelik, A.İ.; Özkılıç, Y.O.; Zeybek, Ö.; Özdöner, N.; Tayeh, B.A. Performance Assessment of Fiber-Reinforced Concrete Produced with Waste Lathe Fibers. *Sustainability* **2022**, *14*, 11817. [[CrossRef](#)]
42. Aksoylu, C.; Özkılıç, Y.O.; Arslan, M.H. Mechanical Steel Stitches: An Innovative Approach for Strengthening Shear Deficiency in Undamaged Reinforced Concrete Beams. *Buildings* **2022**, *12*, 1501. [[CrossRef](#)]
43. Prakash, R.; Thenmozhi, R.; Raman, S.N.; Subramanian, C. Characterization of eco-friendly steel fiber-reinforced concrete containing waste coconut shell as coarse aggregates and fly ash as partial cement replacement. *Struct. Concr.* **2019**, *21*, 437–447. [[CrossRef](#)]
44. Prakash, R.; Divyah, N.; Srividhya, S.; Avudaiappan, S.; Amran, M.; Naidu Raman, S.; Guindos, P.; Vatin, N.I.; Fediuk, R. Effect of Steel Fiber on the Strength and Flexural Characteristics of Coconut Shell Concrete Partially Blended with Fly Ash. *Materials* **2022**, *15*, 4272. [[CrossRef](#)]
45. Srividhya, S.; Vidjeapriya, R.; Neelamegam, M. Enhancing the performance of hyposludge concrete beams using basalt fiber and latex under cyclic loading. *Comput. Concr.* **2021**, *28*, 93. [[CrossRef](#)]
46. Adetukasi, A.O. Strength and deflection characteristics of concrete reinforced with steel swarf. *IOP Conf. Ser. Mater. Sci. Eng.* **2019**, *640*, 012044. [[CrossRef](#)]
47. Sharba, A.A.K.; Ibrahim, A.J. Evaluating the use of steel scrap, waste tiles, waste paving blocks and silica fume in flexural behavior of concrete. *Innov. Infrastruct. Solut.* **2020**, *5*, 94. [[CrossRef](#)]
48. Balea, A.; Fuente, E.; Monte, M.C.; Blanco, A.; Negro, C. Recycled Fibers for Sustainable Hybrid Fiber Cement Based Material: A Review. *Materials* **2021**, *14*, 2408. [[CrossRef](#)]
49. Merli, R.; Preziosi, M.; Acampora, A.; Lucchetti, M.C.; Petrucci, E. Recycled fibers in reinforced concrete: A systematic literature review. *J. Clean. Prod.* **2020**, *248*, 119207. [[CrossRef](#)]
50. Altera, A.Z.A.; Bayraktar, O.Y.; Bodur, B.; Kaplan, G. Investigation of the Usage Areas of Different Fiber Reinforced Concrete. *Kast. Univ. J. Eng. Sci.* **2021**, *7*, 7–18.
51. Yang, E.H.; Wang, S.; Yang, Y.; Li, V.C. Fiber-bridging constitutive law of engineered cementitious composites. *J. Adv. Concr. Technol.* **2008**, *6*, 181–193. [[CrossRef](#)]
52. Özkılıç, Y.O.; Aksoylu, C.; Arslan, M.H. Experimental and numerical investigations of steel fiber reinforced concrete dapped-end purlins. *J. Build. Eng.* **2021**, *36*, 102119. [[CrossRef](#)]
53. Karalar, M.; Özkılıç, Y.O.; Deifalla, A.F.; Aksoylu, C.; Arslan, M.H.; Ahmad, M.; Sabri, M.M.S. Improvement in Bending Performance of Reinforced Concrete Beams Produced with Waste Lathe Scraps. *Sustainability* **2022**, *14*, 12660. [[CrossRef](#)]
54. Neeraja, D.; Arshad, S.M.; Nadaf, A.K.N.; Reddy, M.K. Evaluation of workability and strength of green concrete using waste steel scrap. *IOP Conf. Ser. Mater. Sci. Eng.* **2017**, *263*, 032013. [[CrossRef](#)]
55. Shewalul, Y.W. Experimental study of the effect of waste steel scrap as reinforcing material on the mechanical properties of concrete. *Case Stud. Constr. Mater.* **2021**, *14*, e00490. [[CrossRef](#)]
56. Gemi, L.; Madenci, E.; Özkılıç, Y.O. Experimental, analytical and numerical investigation of pultruded GFRP composite beams infilled with hybrid FRP reinforced concrete. *Eng. Struct.* **2021**, *244*, 112790. [[CrossRef](#)]
57. Arslan, M.H.; Yazman, Ş.; Hamad, A.A.; Aksoylu, C.; Özkılıç, Y.O.; Gemi, L. Shear strengthening of reinforced concrete T-beams with anchored and non-anchored CFRP fabrics. *Structures* **2022**, *39*, 527–542. [[CrossRef](#)]

58. Qureshi, Z.N.; Mushtaq Raina, Y.; Mohd, S.; Rufaie, A. Strength Characteristics Analysis of Concrete Reinforced with Lathe Machine Scrap. *Int. J. Eng. Res. Gen. Sci.* **2016**, *4*, 210–217.
59. ASTM. *Standard Practice for Making and Curing Concrete Test Specimens in the Field*; ASTM International: West Conshohocken, PE, USA, 2012. [[CrossRef](#)]

**Disclaimer/Publisher's Note:** The statements, opinions and data contained in all publications are solely those of the individual author(s) and contributor(s) and not of MDPI and/or the editor(s). MDPI and/or the editor(s) disclaim responsibility for any injury to people or property resulting from any ideas, methods, instructions or products referred to in the content.